On the Reasons for High Activity of CeO_2 Catalyst for Soot Oxidation

Masato Machida,* Yuichiro Murata, Kouji Kishikawa, Dongjie Zhang, and Keita Ikeue

Department of Nano Science and Technology, Graduate School of Science and Engineering, Kumamoto University, 2-39-1 Kurokami, Kumamoto, 860-8555 Japan

Received March 21, 2008. Revised Manuscript Received April 28, 2008

The present work has demonstrated the reasons why CeO_2 becomes an active catalyst for diesel particulate (soot) abatement, which attracts recent worldwide attention in the development of clean diesel automobiles. Four typical fluorite-type oxides, CeO_2, ZrO_2, Pr_6O_{11}, and a CeO_2-ZrO_2 solid solution have been studied as model catalysts for soot oxidation in conjunction with the redox property and the reactivity of solid oxygen species. It was found that the redox property measured in terms of oxygen storage/release capacity was not the sole determining factor for the observed catalytic activity decreasing in the order of $CeO_2 \gg Pr_6O_{11} \approx CeO_2-ZrO_2 > ZrO_2$. The reactivity of oxygen species involved in the redox cycles would rather be important. The ESR measurement showed that admission of O_2 to the pre-reduced CeO_2 surface generated superoxide ions (O_2^-). Such reactive oxygen species were less abundant on CeO_2-ZrO_2 and were not detected on ZrO_2 and Pr_6O_{11}. The labeled and unlabeled O_2 pulse experiments demonstrated that reactive oxygen species on pre-reduced CeO_2 caused a temporal oxidation of soot even at quite a low temperature of 150 °C, compared to more than 350 °C required for successive catalytic soot oxidation. The reactive oxygen is formed from gaseous O_2 adsorbed at the three-phase boundary between soot, reduced CeO_2, and the gas phase, but another active oxygen species, which is formed from the lattice oxygen at the CeO_2/soot interface, contributes much more to the total soot oxidation. Silver loading onto CeO_2 enhanced further the generation of superoxide and thus the catalytic activity for soot oxidation.

Introduction

Diesel automobiles have increased their market share in the world because of their lower fuel consumptions and thus lower CO_2 emissions in comparison to gasoline-fueled automobiles. This situation also causes the strong demand for the diesel particulate abatement by means of after-treatment technology, so-called diesel particulate filter (DPF).[1–11] Conventional DPF requires periodic regeneration to prevent the accumulation of soot in the filter, which causes unacceptable levels of back pressure in the gas exhaust line. However, continuous regeneration assisted by the oxidation catalyst is considered as a more advanced system. A great number of studies have therefore been devoted to developing the active soot oxidation catalyst in the last 2 decade. Many researchers have reported that CeO_2-based oxides have excellent activity for soot oxidation at the lowest possible temperatures.[12–19] However, fundamental understanding of the high activity of CeO_2 for soot oxidation is not established in the open literature.

CeO_2 has been widely used for automotive catalysts as an oxygen-storage component (CeO_2-ZrO_2) in three-way catalysts. The oxygen storage capacity (OSC) due to redox between Ce^{4+} and Ce^{3+} is able to store oxygen under an oxidizing atmosphere and release it under a reducing atmosphere. Aneggi et al.[17] reported the role of oxygen storage in soot oxidation. They explained soot oxidation activity in terms of a simple reduction/oxidation of oxide catalysts analogous to catalytic CO oxidation. The catalytic activity of CeO_2 is therefore considered mainly to be related to the OSC. In contrast, Makkee and co-workers,[2,3,7,8,18,19]

* To whom correspondence should be addressed. Tel./Fax: +81-96-342-3651. E-mail: machida@chem.kumamoto-u.ac.jp.

(1) Ahlström, A. F.; Odenbrand, C. U. I. *Appl. Catal.* **1990**, *60*, 143.
(2) Mul, G.; Neeft, J. P. A.; Kapteijn, F.; Makkee, M.; Moulijn, J. A. *Appl. Catal., B* **1995**, *6*, 339.
(3) Neeft, J. P. A.; Makkee, M.; Moulijn, J. A. *Appl. Catal., B* **1996**, *8*, 57.
(4) Teraoka, Y.; Kagawa, S. *Catal. Surv. Jpn.* **1998**, *2*, 155.
(5) Badini, C.; Saracco, G.; Serra, V.; Specchia, V. *Appl. Catal., B* **1998**, *18*, 137.
(6) Querini, C. A.; Ulla, M. A.; Requejo, F.; Sorai, J.; Sedron, U. A.; Miro, E. E. *Appl. Catal., B* **1998**, *15*, 5.
(7) Jelles, J.; van Setten, B. A. A. L.; Makkee, M.; Moulijn, J. A. *Appl. Catal., B* **1999**, *21*, 35.
(8) van Setten, B. A. A. L.; Makkee, M.; Moulijn, J. A. *Catal. Rev.* **2001**, *43*, 489.
(9) Uchisawa, J. O.; Wang, S.; Nanba, T.; Ohi, A.; Obuchi, A. *Appl. Catal., B* **2003**, *44*, 207.
(10) Fino, D.; Fino, P.; Saracco, G.; Specchia, V. *Appl. Catal., B* **2003**, *43*, 243.
(11) Steenwinkel, Y. Z.; Castricum, H. L.; Beckers, J.; Eiser, E.; Bliek, A. *J. Catal.* **2004**, *221*, 523.
(12) Pisarello, M. L.; Milt, V.; Peralta, M. A.; Querini, C. A.; Miro', E. E. *Catal. Today* **2002**, *75*, 465.
(13) Miro', E. E.; Ravelli, F.; Ulla, M. A.; Cornaglia, L. M.; Querini, C. A. *Catal. Today* **1999**, *53*, 631.
(14) Neri, G.; Rizzo, G.; Galvagno, S.; Musolino, M. G.; Donato, A.; Pietropaolo, R. *Thermochim. Acta* **2002**, *381*, 165.
(15) Courcot, D.; Pruvost, C.; Zhilinskaya, E. A.; Aboukais, A. *Kinet. Catal.* **2004**, *45*, 580.
(16) Pruvost, C.; Lamonier, J. F.; Courcot, D.; Abi-Aad, E.; Aboukais, A. *Stud. Surf. Sci. Catal.* **2000**, *130*, 2159.
(17) Aneggi, E.; de Leitenburg, C.; Dolcetti, G.; Trovarelli, A. *Catal. Today* **2006**, *114*, 40–47.
(18) Setiabudi, A.; Chen, J.; Mul, G.; Makkee, M.; Moulijn, J. A. *Appl. Catal., B* **2004**, *51*, 9.
(19) Krishna, K.; Bueno-Lopes, A.; Makkee, M.; Moulijn, J. A. *Appl. Catal., B* **2007**, *75*, 189.

10.1021/cm800832w CCC: $40.75
Published on Web 06/11/2008

who have conducted comprehensive studies for the development of soot oxidation catalysts from the 1990s, suggested that the bulk OSC is not crucial in determining the soot oxidation activity but the active oxygen transfer to soot is rather important. According to their latest work,[19] the role of CeO_2 is to cause spillover of active oxygen onto the soot surface and its subsequent adsorption at the active carbon site is an intermediate step in the soot oxidation mechanism. They implied that the active oxygen possibly exists in the form of peroxide or superoxide.[18] However, these oxygen radicals have not been detected under real soot oxidation conditions.

In this paper, oxygen species and its storage/release property of four types of fluorite-type oxides, CeO_2, ZrO_2, Pr_6O_{11}, and CeO_2-ZrO_2 solid solution, have been studied with the intention of elucidating the nature of active oxygen species and their physicochemical behaviors in the determination of soot oxidation activity. The catalytic activity was also evaluated in the presence of metal to enhance the generation of active oxygens responsible for the soot oxidation at lower temperatures. Possible reasons for high activity of CeO_2 for soot oxidation have been proposed and discussed to develop a basic material concept for designing active soot combustion catalysts.

Experimental Section

Preparation and Characterization. The oxide catalysts having similar surface areas (20−45 $m^2 \cdot g^{-1}$) were prepared by precipitation from aqueous solutions of nitrates as was reported in our previous report.[20,21] Dropwise addition of aqueous ammonia to the solution of metal nitrates produced precipitates, which were evaporated to dryness and subsequently calcined at 450 °C for 5 h in air. CeO_2-supported metal catalysts were prepared by a simple impregnation method using aqueous solutions of $AgNO_3$, $Pd(NO_3)_2$, $Pt(NO_2)_2(NH_3)_2$, and $Rh(NO_3)_3$, followed by calcination in air at 450 °C for 2 h.

The crystal structure was identified by use of a powder X-ray diffractometer (XRD, Rigaku, Multiflex) with monochromated Cu Kα radiation (30 kV, 40 mA). Energy-dispersive X-ray fluorescence analysis (XRF, Horiba, MESA-500W) was used to determine the chemical composition. The BET surface area was calculated from N_2 adsorption isotherms measured at −196 °C (Bel Japan, Belsorp).

The ESR measurements were performed on a JEOL TE200 spectroscope operating in the X-band. A Mn^{2+} standard was used for frequency calibration. The sample (100 mg) was introduced into a spectroscopic quartz probe cell, which was connected to a conventional high-vacuum line. Prior to the measurement, the sample was reduced in a flow of 5% H_2/He at 500 °C for 1 h and then cooled to −196 °C. The sample was outgassed and then exposed to 2.5% O_2/He (100 kPa), followed by short evacuation. After measuring the spectra at −196 °C, the sample was warmed up to room temperature, where a second measurement was carried out. The spectra were recorded at 9.6 GHz microwave frequency, 200−1000 mW microwave power, 100 kHz modulation frequency, and 1 G modulation amplitude. No significant signal saturation was observed in those conditions.

Redox Characteristics. Dynamic reduction−oxidation cycles were studied by use of a microbalance (TG, Rigaku 8120), which is connected to a dual-gas supplying system. A sample (10 mg) was first heated in a stream of N_2 up to 700 °C, where the constant weight was attained within 30 min. Then the gas feed to the sample was switched between 1.4% H_2 and 30% O_2 balanced by N_2 at every 10 min with recording of the sample weight at this temperature. During the measurement, N_2 was flowed through the balance chamber to protect the weighing mechanism.

Table 1. Soot Oxidation Activity of Fluorite-Type Oxides

	surface area ($m^2 \cdot g^{-1}$)	20% O_2/N_2		N_2	
		T_i[a] (°C)	Δ[b] (μV)	T_i[a] (°C)	Δ[b] (μV)
CeO_2	45	347	500	362	45
ZrO_2	24	483	50	552	30
CeO_2-ZrO_2	40	448	100	449	25
Pr_6O_{11}	20	444	350	448	30

[a] Onset temperature of soot oxidation. [b] Peak exotherm measured by DTA.

Catalytic Soot Oxidation. The catalytic activity for soot oxidation was determined using commercially available carbon black powders (Mitsubishi Chemical Corporation, MA7; surface area 115 $m^2 \cdot g^{-1}$, average particle size 24 nm) as model diesel soot. The soot and catalyst with a weight ratio of 1/20 or 1/4 were ground in an agate mortar for 4 min to obtain so-called tight-contact mixtures. The catalytic test was carried out with gravimetric thermal analysis (TG/DTA, Rigaku 8120). The soot/catalyst mixture (10 mg) was heated in a stream of 20% O_2 balanced with N_2 (20 $cm^3 \cdot min^{-1}$) at a constant rate of 10 °C·min^{-1}. The onset temperature for soot oxidation (T_i) can be determined from the intercept of a linear fit to the observed weight decrease with the zero line. The maximum intensity of the exothermic DTA peak (Δ) was used as another measure, which corresponds to the highest oxidation rate. The catalytic test was also carried out in a conventional flow reactor. The sample (0.1 g) of the soot/catalyst mixtures with a weight ratio of 1/20 was placed in a quartz container. During the heating at the rate of 10 °C·min^{-1}, gaseous mixtures of 10% O_2 and N_2 balance were fed to the sample (200 $cm^3 \cdot min^{-1}$). The effluent gas was analyzed by nondispersive infrared (NDIR) CO/CO_2 analyzers (Horiba VIA510).

The structural change of catalysts during soot oxidation was studied by in situ XRD measurement using a Rigaku RINT-Ultima diffractometer (Cu Kα, 30 kV, 40 mA) equipped with a high-speed two-dimensional detector, D/teX-25. A soot/CeO_2 tight-contact mixture with a weight ratio of 1/4 was placed in a stream of N_2 or 5% O_2 balanced with N_2 (100 $cm^3 \cdot min^{-1}$) in a temperature-controllable chamber, which was heated at the constant rate of 5 °C·min^{-1}. The XRD pattern was measured every 15 °C with a scan rate of 40 °·min^{-1}. The use of the high-speed detector enables rapid scanning of each XRD pattern ($20° \leq 2\theta \leq 60°$) within 1 min, which is short enough to neglect phase changes occurring during data acquisition.

The reactivity of soot/CeO_2 mixtures to O_2 ($^{16}O_2$ or $^{18}O_2$) was also evaluated in pulse mode reactions. After the reduction or oxidation treatment, the soot/CeO_2 tight-contact mixtures with a weight ratio of 1/20 (0.2 g) was placed in a stream of He at a constant temperature of 150−300 °C, where a certain amount of O_2 was injected repeatedly into the stream just before the soot/CeO_2 mixture. The product gas species in the effluent was monitored by using a mass spectrometer (Omnistar, Pfeiffer).

Results and Discussion

The catalytic activities of four fluorite-type oxides, ZrO_2, CeO_2, Pr_6O_{11}, and CeO_2-ZrO_2, for soot oxidation are compared in Table 1. Heating soot alone in 20% O_2/N_2 at a

(20) Machida, M.; Uto, M.; Kurogi, D.; Kijima, T. *Chem. Mater.* **2000**, *12*, 3158.
(21) Machida, M.; Kurogi, D.; Kijima, T. *Chem. Mater.* **2000**, *12*, 3165.

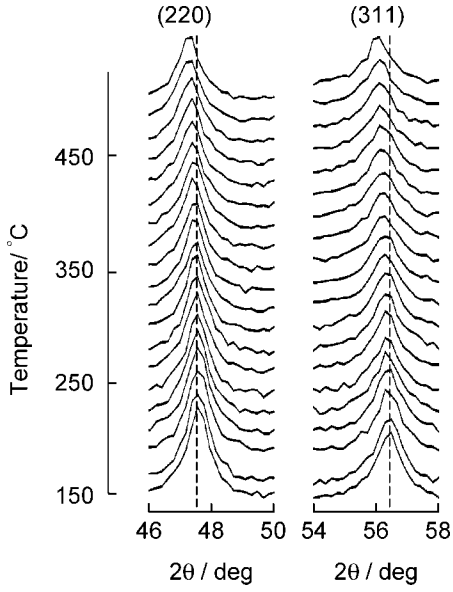

Figure 1. In situ XRD of soot/CeO_2 tight-contact mixtures with weight ratio of 1/4 measured during heating at the rate of 5 °C·min^{-1} in a flow of N_2.

constant rate (10 °C·min^{-1}) showed the onset temperature of soot oxidation, $T_i = 624$ °C, which could be considerably reduced to 347 °C by mixing with CeO_2. The other oxides showed higher T_i and lower Δ; the catalytic activity is thus in the order $CeO_2 \gg Pr_6O_{11} \approx CeO_2-ZrO_2 > ZrO_2$. Because almost the same T_i values were obtained for the different soot/oxide ratios (1/4 and 1/20), the results reflect reaction kinetics under the present test conditions. The high catalytic activity of CeO_2 in tight contact with soot is in accordance with a number of previous studies.[12–19] Soot oxidation was also carried out in the stream of N_2. It should be noted that only small changes of T_i were observed for CeO_2, Pr_6O_{11}, and CeO_2-ZrO_2, whereas ZrO_2 required much higher T_i of 552 °C, compared to 483 °C in the presence of O_2. Very low exotherms (Δ) in the absence of O_2 is consistent with slow soot oxidation under anaerobic conditions, where lattice oxygens of each catalyst were consumed mainly by the soot oxidation.

To confirm that lattice oxygens participate in the soot oxidation, in situ XRD measurement was performed on tight-contact mixtures of soot/CeO_2 with a weight ratio of 1/4 measured in a flow of N_2. Figure 1 shows changes of the (220) and (311) reflections of CeO_2 during heating at a constant rate of 5 °C·min^{-1}. Although the diffraction pattern assigned to the fluorite-type structure was retained, the shift of each peak toward lower 2θ occurred above 350 °C, the temperature at which the soot oxidation started as shown in Table 1. The shift can be explained by the lattice expansion caused by the partial reduction of Ce^{4+} to Ce^{3+} accompanied by the creation of oxygen vacancies. When the measurement was carried out in the presence of O_2, no such shift was observed because the vacancy should immediately be filled by oxygen supplied from the gas phase.

These results imply that release/storage of oxygen is one plausible factor determining the catalytic activity for soot oxidation. Figure 2 displays the weight changes during dynamic oxygen release/storage of the four fluorite-type

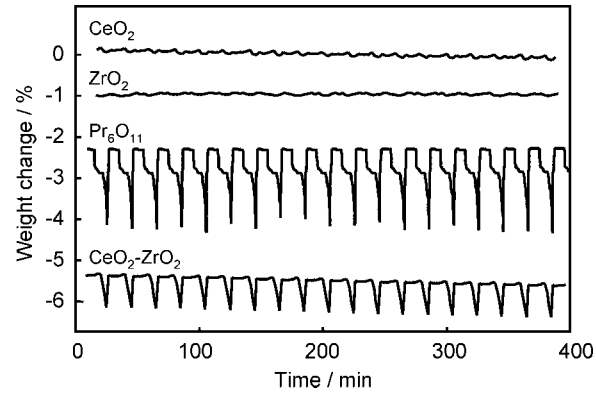

Figure 2. Weight changes of CeO_2, ZrO_2, Pr_6O_{11}, and $CeO-ZrO_2$ under cycled feed streams of 30% O_2 and 1.4% H_2 at 700 °C.

oxides under a cycled feed-stream condition (30% O_2/N_2 or 1.4% H_2/N_2, 10 min intervals) at 700 °C. The oxygen storage capacity (OSC) can be estimated from the amplitude of weight oscillations. Negligible weight change for ZrO_2 is consistent with the lack of redox property. CeO_2 exhibited the weight oscillation, but the small amplitude implies redox mainly near the solid surface. By contrast, the CeO_2-ZrO_2 solid solution showed much larger amplitudes corresponding to about 0.07 mol of O_2·mol of Ce^{-1}, which is about 28% of theoretical OSC ($CeO_2 \rightarrow CeO_{1.5}$; 0.25 mol of O_2·mol of Ce^{-1}). The largest amplitude was attained by Pr_6O_{11}; the OSC of 0.11 mol of O_2·mol of Pr^{-1} is about 65% of the theoretical value ($Pr_6O_{11} \rightarrow 3Pr_2O_3$; 0.17 mol of O_2·mol of Pr^{-1}). The lattice oxygens of these three oxides may take part in the soot oxidation as discussed above. However, CeO_2 is much more active for soot oxidation than Pr_6O_{11} and CeO_2-ZrO_2, having larger OSCs (Table 1). These results suggest that the large OSC does not seem to be essential for catalytic soot oxidation. The reactivity rather than quantity of oxygen species involved in oxygen release/storage processes would rather be an important factor to achieve the soot oxidation at the lowest temperatures.

To elucidate the nature of oxygen species formed during redox cycles, the ESR spectra of the four fluorite-type oxides were measured after reduction in 5% H_2/He at 500 °C and subsequent admission of 2.5% O_2/He (100 kPa) at −196 °C. As shown in Figure 3, CeO_2 yielded very intense signals at $g = 2.04$, 2.02, and 2.01 typical of superoxide radical ions (O_2^-) as was reported by many researchers so far.[22–27] These signals were stable at −196 °C for several 10 min, but their intensity decreased instantly with an increase of temperature to 25 °C. CeO_2-ZrO_2 yielded similar but less intense signals, the line shapes of which were significantly broadened. No such ESR signals were found for Pr_6O_{11} and ZrO_2. Figure 4(a) exhibits the spectrum of the soot/CeO_2 tight-contact mixture after heating at 500 °C in a flow of N_2. With an

(22) Zhang, X.; Klabunde, K. J. *Inorg. Chem.* **1992**, *31*, 1706.
(23) Abi-Aad, E.; Bechara, R.; Grimblot, J.; Aboukais, A. *Chem. Mater.* **1993**, *5*, 793.
(24) Haneda, M.; Mizushima, T.; Kakuta, N. *J. Chem. Soc., Faraday Trans.* **1995**, *91*, 4459.
(25) Soria, J.; Martínez-Arias, A.; Conesa, J. C. *J. Chem. Soc., Faraday Trans.* **1995**, *91*, 1669.
(26) Soria, J.; Coronado, J. M.; Conesa, J. C. *J. Chem. Soc., Faraday Trans.* **1996**, *92*, 1619.
(27) Martínez-Arias, A.; Coronado, J. M.; Cataluna, R.; Conesa, J. C.; Soria, J. *J. Phys. Chem. B* **1998**, *102*, 4357.

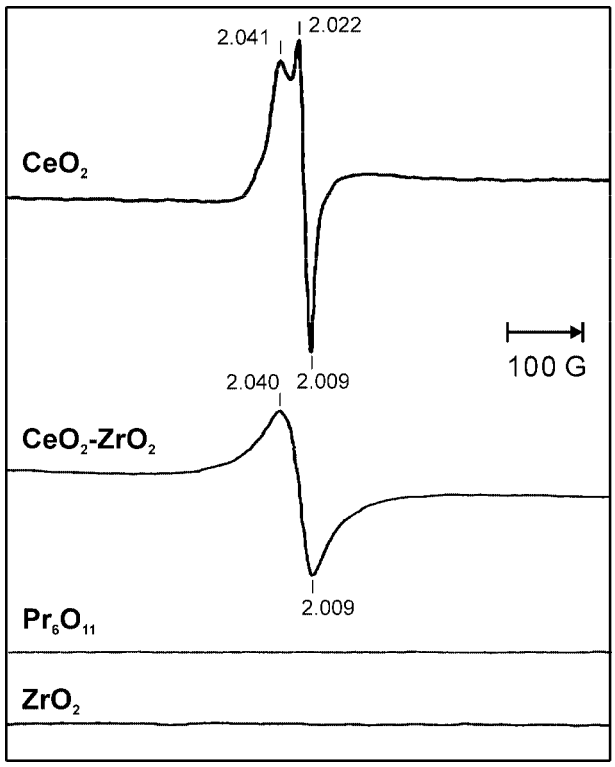

Figure 3. ESR spectra of four fluorite-type oxide taken at −196 °C after reduction by H_2 at 500 °C and subsequent exposure to 2.5% O_2/He at −196 °C.

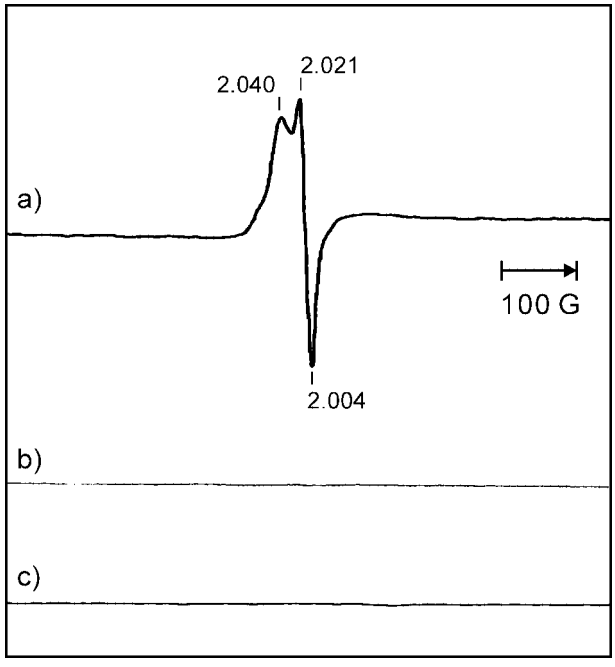

Figure 4. ESR spectra taken at −196 °C after exposure to 2.5% O_2/He at −196 °C. (a) Soot/CeO_2 tight-contact mixtures with weight ratio of 1/20 after heating in N_2 at 500 °C, (b) CeO_2 after heating in N_2 at 500 °C, and (c) soot/CeO_2 tight-contact mixtures with weight ratio of 1/20 after heating in air at 500 °C.

admission of 2.5% O_2/He at −196 °C, signals due to the superoxide appeared as in Figure 3. By contrast, the signal did not appear when CeO_2 alone was heated in N_2 (b) or when the soot/CeO_2 tight-contact mixture was heated in air (c). These results clearly suggest that superoxide radicals will possibly be formed on CeO_2 in the soot oxidation processes, when oxygen is admitted to the reduced surface of CeO_2.

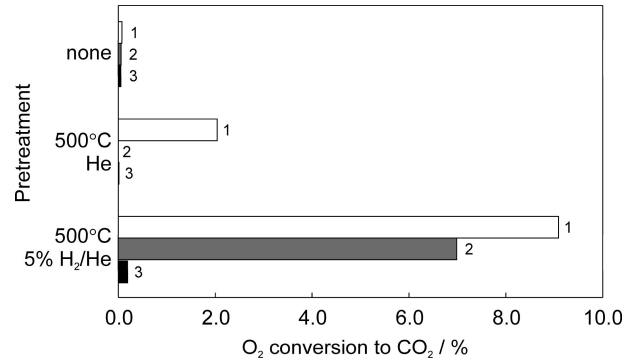

Figure 5. O_2 pulse reactions at 150 °C after different pretreatment of soot/CeO_2 tight-contact mixtures with weight ratio of 1/20. The number of pulses is shown along each bar.

The ease of superoxide formation is in accordance with the highest soot oxidation activity of CeO_2. The superoxide species are able to be detected by means of ESR and/or Raman spectroscopy only at low temperatures. Unfortunately, however, it is difficult to detect this species under the real reaction conditions because their lifetime should be very short; superoxides formed on the surface of CeO_2 should immediately react with carbon in the vicinity or recombine to generate O_2.

The generation of active oxygen species in soot oxidation was next evaluated by the method of micropulse injection of O_2. In this experiment, the soot/CeO_2 tight-contact mixture after different treatments was placed in flowing He at 150 °C, which is quite lower than the onset temperatures, $T_i \geq$ 350 °C, shown in Table 1. An injection of 1.6 cm^3 of O_2 into the gas feed was repeated with monitoring the mass spectra of the effluent to detect the species coming from the mixture, which were mainly composed of O_2 and CO_2. Figure 5 shows the conversion of O_2 to CO_2 for the first three pulses. The O_2 reaction with untreated soot/CeO_2 mixtures was negligible. When the mixture was preheated at 500 °C in He, however, only the first O_2 pulse produced a small amount of CO_2 (2% O_2 conversion). More significant CO_2 evolution was observed for the mixture after reduction in 5% H_2/He at 500 °C. It should be noted that more than 9% of the first O_2 injection could be utilized to oxidize soot to CO_2 at quite a low temperature of 150 °C, compared to that at about 350 °C requested for successive oxidation of soot as shown in Table 1. This is an indication of the high reactivity of oxygen adsorbed onto the reduced CeO_2. It should be noted that oxygen in first and second injections was consumed not only by the soot oxidation but also by the reoxidation of CeO_2, simultaneously. Therefore, the soot oxidation is temporal and the active oxygen species would disappear steeply by repeating further the injection of O_2 pulses because the reoxidation of CeO_2 is completed. When CeO_2 alone was used in place of the soot/CeO_2 mixture, O_2 pulses were consumed only by the reoxidation.

Micropulse reactions were also carried out using an oxygen isotope $^{18}O_2$ with a view to elucidate the fate of O_2 injected onto the prereduced CeO_2/soot mixture, that is, to identify whether the isotope oxygen comes into the CeO_2 lattice or directly reacts with soot to produce CO_2. The *m*/*e* values, characteristic of the various species measured by a mass

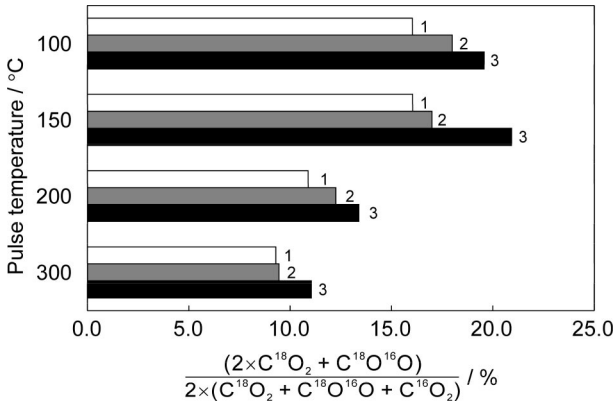

Figure 6. Isotope fractions in product CO_2 for $^{18}O_2$ pulse reactions at different temperatures. A soot/CeO_2 tight-contact mixture with weight ratio of 1/20 was used after reduction in 5% H_2/He at 500 °C. The number of pulses is shown along each bar.

spectrometer, were chosen as 28($C^{16}O$), 30($C^{18}O$), 32($^{16}O_2$), 34($^{16}O^{18}O$), 36($^{18}O_2$), 44($C^{16}O_2$), 46($C^{16}O^{18}O$), and 48($C^{18}O_2$). The injection of $^{18}O_2$ yielded $C^{16}O_2$, $C^{16}O^{18}O$, and $C^{18}O_2$ as primary products of soot oxidation, but signals of $C^{16}O$ and $C^{18}O$ were negligibly small. Isotope oxygen equilibration between the gas phase and the solid can be neglected at ≤300 °C judging from the trace amount of $^{16}O_2$ and $^{16}O^{18}O$ in the effluent. Figure 6 exhibits the isotope fraction in the product CO_2 for pulse reactions at different temperatures. At 150 °C, the oxygen in the product CO_2 contained 16% of ^{18}O, implying the occurrence of soot oxidation by adsorbed oxygen species, which are supplied from the gas phase. However, it should rather be noted that the rest (84%) of oxygen in the product CO_2 originated from the CeO_2 lattice even after the reduction treatment. The isotopic fraction increased with the number of pulses. This is simply because the reduced CeO_2 is reoxidized by $^{18}O_2$ so that more ^{18}O species penetrate into the bulk with the progress of pulsing as evident from a very high rate of oxygen transport within the lattice of reduced CeO_2. Also, the isotope fraction tends to decrease with an increase of temperature, suggesting that more lattice oxygens come into play as active species at increasing temperatures.

Considering these results described above, two possible reaction pathways can be proposed. One pathway may include the formation of active oxygens, superoxide (O_2^-), via oxygen adsorption onto the reduced surface of CeO_2 in the vicinity of soot and subsequent electron transfer from surface donor (Ce^{3+}) as follows:[28,29]

$$Ce^{3+}-V_O + O_2 \rightarrow Ce^{4+}-(O-O)^- \quad (V_O\text{: oxygen vacancy})$$

Such defects can promote the activation of adsorbed oxygen to form superoxides even in the lattice. Filimonov and co-workers[30] reported that the fluorite-type structure of CeO_2 plays a key role in accommodating the oxygen radicals inside the lattice. A possible site for superoxide stabilization is assumed to be a central empty octahedron inside the fluorite-type lattice. The reason for highly efficient formation of superoxide anions in CeO_2 may be explained by the moderate redox property of cerium. ZrO_2 cannot yield this oxygen species because of the lack of redox ability. By contrast, praseodymium oxide, having the highest redox ability among the present four fluorite-type oxides, can reduce immediately adsorbed neutral dioxygen (O_2) to inert lattice oxide anion (O^{2-}) in the sequence $O_2 \rightarrow O_2^- \rightarrow O_2^{2-} \rightarrow 2O^- \rightarrow 2O^{2-}$.

In the soot oxidation process, soot plays the role of a reducing agent for CeO_2 as was demonstrated in Figure 5. The resulting reduced surface would cause oxygen adsorption, at around the three-phase boundary between soot, CeO_2, and the gas phase, to form the superoxide species, which nexts react with soot in the vicinity to form carbon dioxide,

$$2[Ce^{4+}-(O-O)^-] + C \rightarrow 2[Ce^{4+}-O] + CO_2$$

The present results demonstrated the extremely high reactivity of these species toward soot oxidation even at a low temperature of 150 °C as shown in Figure 5. However, the reaction should soon be stopped at this temperature because superoxide anions will not be generated when the reoxidation of CeO_2 is complete. This accounts for the lower catalytic activity of oxidized CeO_2 compared to reduced ones. Above the onset temperature (T_i, ≥350 °C), soot/CeO_2 reactions should generate a number of $Ce^{3+}-V_O$ at the three-phase boundary, followed by adsorption of molecular oxygen to regenerate reactive oxygens. In this way, the successive soot oxidation would proceed very rapidly.

Another possible reaction pathway, which was found to be more important for soot oxidation, is the reaction between soot and active lattice oxygens at the soot/CeO_2 interface as was indicated by Figure 6. Although the nature of this lattice oxygen species is not well-known, spontaneous reactions with soot are driven as a result of the O_2 uptake by prereduced CeO_2. This may be explained if the sorption of O_2 would induce the activation of lattice oxygen existing at the soot/CeO_2 interface (O_i) as shown in the following example,

$$^1/_2O_2 + V_O + O^{2-}{}_i \rightarrow O^- + O^-{}_i$$

Unfortunately, we do not have any experimental evidence for such pathways, but it is not in conflict with the literature,[30–32] which reported the high reactivity of lattice oxygens in pre-reduced CeO_2 compared to oxidized ones. Holmgren et al.[31] reported that the effect on $CO-O_2$ reaction over Pt/CeO_2 is associated with active oxygens, which come from the lattice and not from the gas phase. This implies that active lattice oxygens would be supplied for catalytic reactions during the reoxidation of pre-reduced CeO_2. However, they also did not reach unambiguous conclusions because the isotope exchange effect in their analysis could not be neglected. Makkee and co-workers[32] have also carried out soot oxidation with an oxygen isotope at a high temperature of 600 °C, where isotopic oxygen exchange between gaseous O_2 and lattice oxygens of CeO_2 was observed, but they concluded that soot oxidation was still being carried out by lattice oxygens.

(28) Li, C.; Domen, K.; Maruya, K. I.; Onishi, T. *J. Am. Chem. Soc.* **1989**, *111*, 7683.
(29) Pushkarev, V. V.; Kovalchuk, V. I.; d'Itri, J. L. *J. Phys. Chem. B* **2004**, *108*, 5341.
(30) Aboukais, A.; Zhilinskaya, E. A.; Lamonier, J. F.; Filimonov, I. L. *Colloids Surf., A* **2005**, *260*, 199.
(31) Holmgren, A.; Azarnoush, F.; Fridell, E. *Appl. Catal., B* **1999**, *22*, 49.
(32) Bueno-López, A.; Krishna, K.; van der Linden, B.; Mul, G.; Moulijn, J. A.; Makkee, M. *Catal. Today* **2007**, *121*, 237.

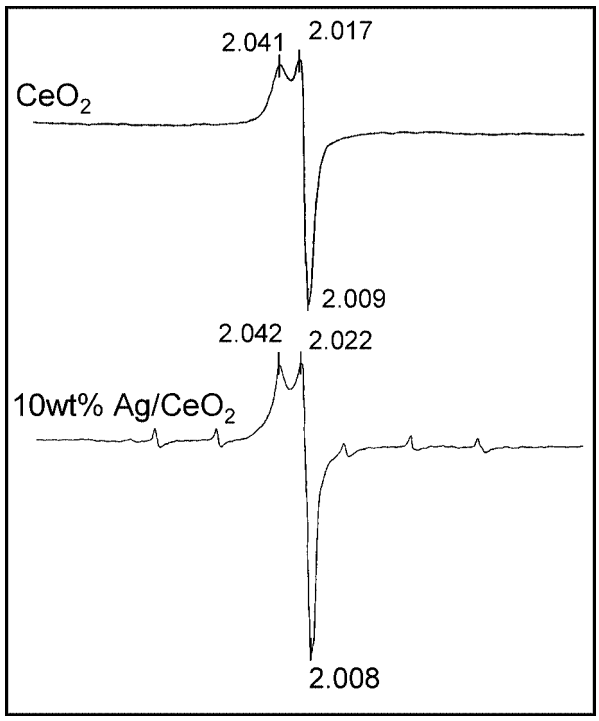

Figure 7. ESR spectra of CeO_2 and 10 wt % Ag/CeO_2 taken after reduction by H_2 at 500 °C and subsequent exposure to 2.5% O_2/He at −196 °C. The weak six signals are ascribable to Mn^{2+} impurity.

Based on these considerations, modification that promotes the formation of active oxygen species is expected to enhance further the soot oxidation activity of CeO_2. We have thus studied the effect of metal loading (Pt, Pd, Rh, and Ag) on CeO_2 and found that Ag is most promising. Figure 7 exhibits the ESR spectra of CeO_2 before and after loading of 10 wt % Ag. The introduction of O_2 after the reduction treatment gave rise to signals ascribable to superoxide, which were intensified by loading Ag. The XRD measurement suggests that the sample consists of metallic silver and CeO_2 and mixed oxide phases could not be detected. It is well-known that a metallic silver surface can promote the formation of superoxide ions (O_2^-).[33–35] These species are molecularly adsorbed in a bent end-on geometry on the silver surface and play a key role in the catalytic epoxidation of ethelene.[36] Also, Villani et al.[37] recently pointed out the potential of silver as an active catalyst for soot oxidation.

Figure 8 shows the effluent gas profiles for 10 wt % Ag loaded and unloaded CeO_2 tightly mixed with soot. The onset of soot oxidation over the Ag loaded CeO_2 was about 50 °C lower than that for unloaded CeO_2. In both cases, CO_2 was a sole product but CO was negligible. Figure 9 compares the onset temperature, T_i, of soot oxidation over various metal-loaded CeO_2 with different loadings. Clearly, T_i can be lowered with an increase of Ag loading from 357 to 324 °C (20 wt %). By contrast, loading other metals, Pd, Pt, and Rh, could not improve the catalytic activity. The result is

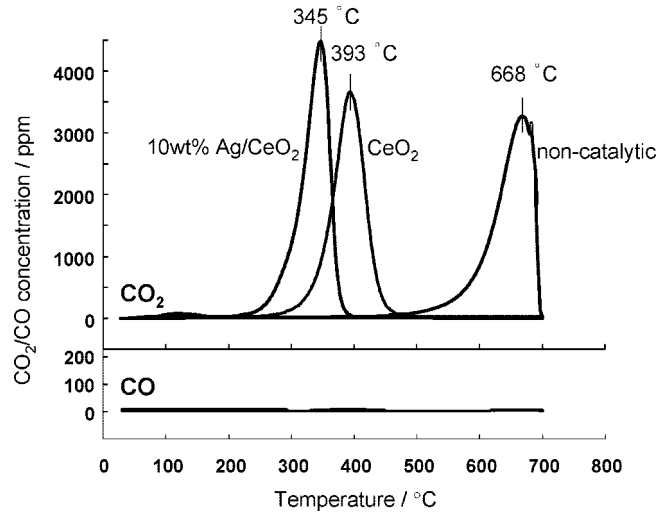

Figure 8. Effect of Ag loading on soot combustion profiles of CeO_2. Soot/CeO_2 tight-contact mixtures with weight ratio of 1/20 were heated in 10% O_2/N_2 at the rate of 10 °C·min^{-1}.

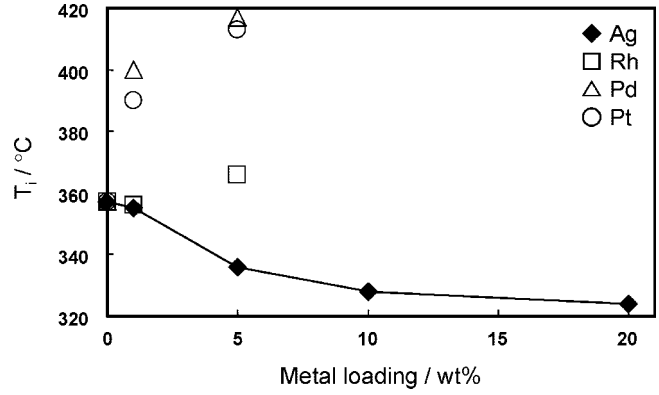

Figure 9. Soot oxidation activity (T_i) of metal-loaded CeO_2 measured in a flow of 10% O_2 and N_2 balance. Tight-contact soot/catalyst mixtures with weight ratio of 1/20 were heated at the rate of 10 °C·min^{-1}.

consistent with the experimental observations described above, supporting the belief that the superoxide is a possible reactive species responsible for low-temperature soot oxidation.

Conclusion

The present work demonstrated the formation of active oxygens for soot oxidation over a reduced CeO_2 surface. CeO_2, having the highest activity for the oxidation of tight-contacting soot, can generate superoxide species most efficiently among the four different fluorite-type oxides (CeO_2, ZrO_2, Pr_6O_{11}, and CeO_2−ZrO_2). Unfortunately, however, these active oxygen species have not been confirmed under real soot oxidation conditions because its lifetime would be too short to be detected above ambient temperature. Instead, the oxygen pulse experiment using $^{16}O_2$ and $^{18}O_2$ could confirm the two possible reaction pathways including active oxygen species: (i) reactions between adsorbed superoxides and soot at the three-phase boundary and (ii) reactions between active lattice oxygen and soot at the CeO_2/soot interface. This idea can broadly be applied to the design of novel active catalytic materials efficient for soot oxidation at lowest possible temperatures.

CM800832W

(33) Shimizu, N.; Shimokoshi, K.; Yasumori, I. *Bull. Chem. Soc. Jpn.* **1973**, *46*, 2929.
(34) Clarkson, R. B. *J. Catal.* **1974**, *33*, 392.
(35) Aboukais, A.; Jarjoui, M.; Verdrine, J. C.; Gravelle, P. C. *J. Catal.* **1977**, *47*, 399.
(36) Tanaka, S.; Yamashina, T. *J. Catal.* **1975**, *40*, 140.
(37) Villani, K.; Brosius, R.; Martens, J. A. *J. Catal.* **2005**, *236*, 172.